# Magnetic Resonance Spectroscopy as a Tool for Assessing Macromolecular Structure and Function in Living Cells

Conggang Li,[1] Jiajing Zhao,[1] Kai Cheng,[1] Yuwei Ge,[1]
Qiong Wu,[1] Yansheng Ye,[1] Guohua Xu,[1]
Zeting Zhang,[1] Wenwen Zheng,[1] Xu Zhang,[1]
Xin Zhou,[1] Gary Pielak,[2] and Maili Liu[1]

[1]Key Laboratory of Magnetic Resonance in Biological Systems, State Key Laboratory of
Magnetic Resonance and Atomic and Molecular Physics, National Center for Magnetic
Resonance, Wuhan Institute of Physics and Mathematics, Chinese Academy of Sciences, Wuhan
430071, China; email: conggangli@wipm.ac.cn, ml.liu@wipm.ac.cn

[2]Department of Chemistry, Department of Biochemistry and Biophysics, and Lineberger
Comprehensive Cancer Center, University of North Carolina, Chapel Hill,
North Carolina 27599

**Abstract**

Investigating the structure, modification, interaction, and function of
biomolecules in their native cellular environment leads to physiologically
relevant knowledge about their mechanisms, which will benefit drug discov-
ery and design. In recent years, nuclear and electron magnetic resonance
(NMR) spectroscopy has emerged as a useful tool for elucidating the struc-
ture and function of biomacromolecules, including proteins, nucleic acids,
and carbohydrates in living cells at atomic resolution. In this review, we sum-
marize the progress and future of in-cell NMR as it is applied to proteins,
nucleic acids, and carbohydrates.

# 1. INTRODUCTION

Biomacromolecules, including proteins, nucleic acids, and polysaccharides, perform many functions essential to life. Almost everything we know about these molecules comes from studying their purified forms in simple buffers. However, most of them perform their function in the crowded and complex cellular environment where biomacromolecules can occupy 30% of the total volume, and their concentrations can exceed 300 g/L (1). These conditions are predicted to have large effects on many properties of biomacromolecules (2). A primary goal of biology is to understand the structure, stability, function, and dynamics of these biomacromolecules in living cells; techniques such as fluorescence and Raman spectroscopies have been applied to study them. Unfortunately, specific fluorescent labeling of target molecule in cells remains challenging, and only their locations and large structural changes can be detected. Recently, nuclear magnetic resonance (NMR) spectroscopy has emerged as a technique to provide atomic-level information about biomacromolecules in their natural environment. This review covers recent advances that use NMR to assess the properties of macromolecules in living cells.

NMR has been applied to small molecule metabolism in living cells almost since this spectroscopy was invented because it is noninvasive (3). Macromolecules, including proteins, DNAs, RNAs, and carbohydrates, which show more complex structure and dynamics than small molecules, are more difficult to study in cells due to the low sensitivity of NMR. To our knowledge, London et al. (4) published the first in-cell protein NMR spectrum in 1975. They showed that histidine resonances from carbonmonoxyhemoglobin could be detected in the combined red blood cells from a dozen mice fed $^{13}$C-enriched histidine. In the same year, Llinas et al. (5) identified peptide resonances in spectra of the fungus *Ustilago sphaerogena* grown in $^{15}$N-enriched ammonium acetate. These two efforts were followed by the 1977 contribution of Daniels et al. (6), who reported the $^{1}$H spectrum of dissected rat adrenal medulla and identified the aliphatic resonances from the 49-kDa protein chromogranin A.

Nevertheless, these groundbreaking papers have been cited only ∼150 times in four decades. The main reason for the paucity of recognition serves as a springboard for this review. The hemoglobin was detectable because it was isotopically enriched at histidine residues. Without specific enrichment (or labeling), globular proteins often do not give rise to high-quality in-cell spectra. Chromogranin A was only visible because it is highly expressed in this cell type, which allows its spectrum to be observed above the background spectra of the other cellular components. Chromogranin A was detectable because it is not a globular protein but is instead intrinsically disordered. Such proteins give sharp resonances because disorder leads to flexibility that is absent from globular proteins (7, 8).

The revolution in molecular biology in the 1970s and 1980s resulted in straightforward protocols for protein overexpression and uniform isotope enrichment or labeling, making it possible to detect one protein in a sea of others. Brindle's group (9) published the first such experiments in 1989. This study involved induction and labeling of the enzyme 3-phosphoglycerate kinase with 5-fluorotryptophan in yeast. A few years later, Dötsch and colleagues (10) pioneered in-cell NMR in *Escherichia coli* by inducing the protein of interest in media containing NMR active nuclei (e.g., $^{15}$N, $^{13}$C) followed by application of heteronuclear multidimensional NMR experiments. Pielak's group (11) obtained high-quality $^{15}$N–$^{1}$H heteronuclear single-quantum correlation (HSQC) spectra of the disordered protein FlgM in *E. coli*. These and other efforts catalyzed the development of a large number of applications aimed at gaining information about structure, interaction, modifications, and function of various biomolecules in various types of cells.

## 2. MAGNETIC RESONANCE STUDIES OF PROTEIN IN CELLS

### 2.1. Protein Structure

High-resolution protein structure is fundamental to understand why protein has certain functions and why some mutations result in malfunction. Among high-resolution structural determination methods, NMR is the only one to provide atomic-resolution structure in solution. Whether the protein structure determined in vitro reflects the real structure in living cells remains a question.

**2.1.1. Solution-state in-cell NMR.** *Thermus thermophilus* HB8 protein TTHA1718 is the first protein whose high-resolution structure was determined in living *E. coli* cells by in-cell NMR (12, 13). Due to the poor resolution and strong background of in-cell spectra, the sample was uniformly $^{13}C/^{15}N$ enriched, and selected side-chain methyl-protonated amino acids (Val/Leu, Ala/Val, and Ala/Leu/Val) were used in an otherwise uniformly enriched $^{2}H$ background. Three-dimensional (3D) spectra with nonlinear sampling (14, 15) in the indirect dimensions were used to make assignments and obtain nuclear Overhauser effect (NOE) distance restraints in times compatible with the life of the cells. The structures were calculated with the program CYANA and energy refined using NOE distance restraints, hydrogen bond distance restraints in regular secondary structure elements, and backbone torsion angle restraints (**Figure 1**).

The structure in cells was essentially identical to that obtained in buffer, which is expected for several reasons. Anfinsen (16) was awarded the Nobel Prize in Chemistry for showing that the 3D structure of a globular protein represents the lowest free-energy state. Richards (17) then showed that the inside of a globular protein is almost as efficiently packed as perfectly packed spheres. If the folded form of a globular protein is most stable, and the inside is efficiently packed, crowding is not expected to change structure.

For disordered proteins or multidomain proteins with more flexibility, the situation might be different. Theillet et al. (18) showed that the intrinsically disordered protein α-synuclein adopts a more compact conformation in mammalian cells than it does in buffer by using paramagnetic
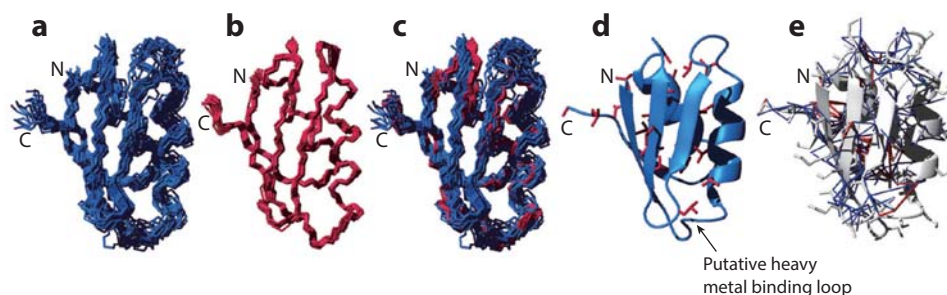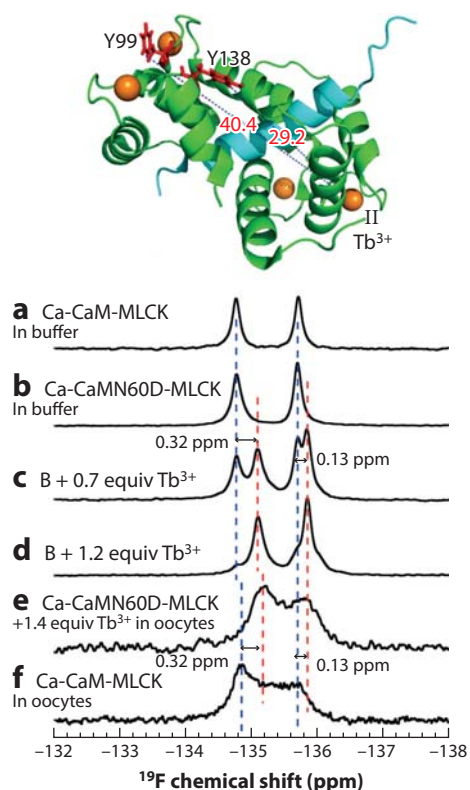


**Figure 1**

NMR solution structure of *Thermus thermophilus* HB8 protein TTHA1718 in living *Escherichia coli* cells. (*a*) Superposition of the 20 final structures of TTHA1718 in living *E. coli* cells, showing the backbone (N, Cα, Cβ) atoms. (*b*) Superposition of the 20 final structures of purified TTHA1718. (*c*) Comparison of structures shown in *a* and *b*. The best-fit superposition of backbone atoms of the two conformational ensembles is shown with the same color code used in *a* and *b*. (*d*) Secondary structure of TTHA1718 in living *E. coli* cells. The side chains of alanine, leucine, and valine residues, the methyl groups of which were labeled with $^{1}H/^{13}C$, shown in red. (*e*) Distance restraints derived from methyl group–correlated and other NOEs are represented in the ribbon model with red and blue lines, respectively. Figure and caption reproduced with permission from Reference 12. Copyright 2009, Nature Publishing Group. Abbreviations: NMR, nuclear magnetic resonance; NOE, nuclear Overhauser effect.
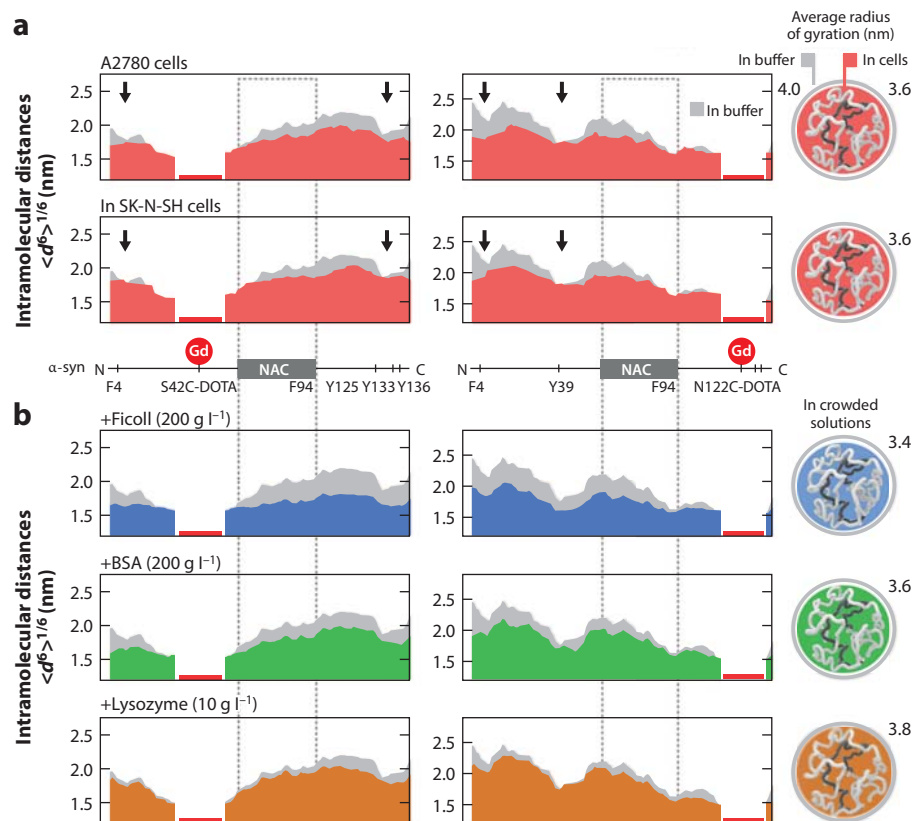
**Figure 2**

(*a*) Intramolecular PRE-derived distance profiles of N-terminally acetylated α-synuclein in buffer (*gray*) and in A2780 and SK-N-SH cells (*red*). (*b*) Comparative PRE-derived distance profiles in (*blue*) Ficoll-, (*green*) BSA- and (*orange*) lysozyme-crowded solutions. Gd(III)-DOTA tags at residues 42 (*left*; S42C-DOTA) and 122 (*right*; N122C-DOTA) provide complementary information about α-synuclein compaction in the respective environments. Proximal PRE effects render residues adjacent to the conjugated Gd(III) invisible (*red bars*). PRE-derived distances were obtained assuming that every Gd(III)-$^1$H vector fluctuation rate scales linearly with that of the backbone N–H vector and the Gd(III)-DOTA complex. For simplification, profiles show values averaged over three consecutively resolved residues. Comparisons of α-synuclein dimensions in buffer, in cells, and in the presence of different crowding agents are shown on the right. Average radii of gyration and levels of α-synuclein compaction are delineated based on the scaling of representative PRE distances relative to values measured in buffer. In the depicted models, residues of the NAC region are colored in dark gray. Arrows denote regions of marked intramolecular contacts. Reproduced with permission from Reference 18. Copyright 2016, Nature Publishing Group. Abbreviations: α-syn, α-synuclein; BSA, bovine serum albumin; NAC, non-amloid-β component; PRE, paramagnetic relaxation enhancement.

relaxation enhancement (PRE) and electron paramagnetic resonance (EPR) spectroscopy (**Figure 2**). PRE effects scale as r$^{-6}$, where r is the distance between the paramagnetic center and nuclear spin, providing abundant distance information that depends on the tumbling time of the protein. By contrast, EPR delivers less information but can be used to measure distances via the PELDOR (19) method independent of the tumbling. These methods are complementary and provide indispensable distance constraints for protein structural measurement. In this study, the

**Figure 3**

(*a*) One-dimensional $^{19}$F NMR spectra of Ca-CaM-MLCK, (*b*) Ca-CaMN60D (asparagine mutated to aspartic acid)-MLCK, and (*c*) Ca-CaMN60D-MLCK in the presence of 0.7 equiv of Tb$^{3+}$, (*d*) 1.2 equiv of Tb$^{3+}$ in buffer, or 1.4 equiv of Tb$^{3+}$ in *Xenopus* oocytes. (*e*) A molar ratio of Ca$^{2+}$ to Ca-MN60D-MLCK of 5:1 and (*f*) diamagnetic Ca-CaM-MLCK in *Xenopus* oocytes. The Ca-CaMN60D-MLCK model is shown at the top (PDB_ID:2LV6). The distances between the $^{19}$F nuclei and the paramagnetic center (II, Tb$^{3+}$) are indicated in red. Figure and caption reproduced with permission from Reference 21. Copyright 2015, Wiley Publishing Group. Abbreviation: NMR, nuclear magnetic resonance.

paramagnetic compound Gd(III)-DOTA was attached to α-synuclein via thioether bonds that withstand the reducing environment of the cytoplasm (20).

Another paramagnetic NMR technology, pseudocontact shift (PCS), provides distance and orientation information and is applied to proteins in cells. Ye et al. (21) were the first to observe $^{19}$F PCS of CaM-MLCK protein in *Xenopus* oocytes by introducing paramagnetic Tb$^{3+}$ into the protein (**Figure 3**). Actually, $^{19}$F PCS only yielded a limited number of PCS values, and it was difficult to draw a conclusion about cellular effects on the whole structure by comparing the in-cell and in vitro values. However, by using these parameters, the authors were able to obtain valuable structural information despite a seriously broadened in-cell $^{15}$N–$^{1}$H HSQC spectrum.

Recently, Pan et al. (22) and Müntener et al. (23) determined the structure of the protein G B1 domain (GB1) in intact *Xenopus* oocytes by using the Rosetta program with PCS restraints. These studies provided a fast and effective way for determining the structures of proteins in living cells. A new carbamidomethyl-linked tag was also designed for measuring PCS restraints in living HeLa cells (24). Combined with proper labeling strategies, NMR methods, and calculation programs,

we predict that more than just model protein structures will be determined in living cells by in-cell NMR (25, 26).

**2.1.2. Solid-state in-cell NMR.** Solution-state NMR will not work with large proteins, membrane proteins, or protein complexes. These situations result in short transverse relaxation times ($T_2$), which cause the broadening or even complete disappearance of resonances. In general, $T_2$ depends on the tumbling rate of the test molecule and decreases with increasing molecular mass and viscosity. Consequently, several high-resolution magic angle spinning (HRMAS) solid-state in-cell NMR methods were developed (27–30) to overcome these predicaments. In magic angle spinning (MAS) solid-state NMR, fast sample rotation is mainly used to remove the resonances broadening from dipolar coupling and chemical shift anisotropy. Recently, dynamic nuclear polarization (DNP) enhancement was employed in HRMAS solid-state in-cell NMR spectroscopy, resulting in an approximately two-order-of-magnitude improvement (27–30) in signal. The technique transfers the high polarization of unpaired electrons to the nuclei of interest using matched microwave irradiation (31). Yamamoto et al. (32) showed that MAS solid-state NMR experiments using DNP were suitable for studying the structure and dynamics of membrane-bound proteins containing a large soluble protein domain. They obtained an approximately 16-fold signal enhancement from $^{13}$C-labeled cytochrome-$b_5$ membrane protein in *E. coli* cells by using AMUPol with a two-dimensional (2D) $^{13}$C-$^{13}$C chemical shift-correlation MAS experiment.

Besides full $^{13}$C- and site-specific ($^{13}$C or $^{15}$N) enrichment (33, 34), $^{13}$C-methyl side chain–enriched and $^{19}$F-labeled proteins open up innovative ways to investigate large macromolecular assemblies and membrane proteins (35). As a nearly 100% natural abundance nucleus, $^{19}$F is often an ideal candidate for monitoring functionally important conformational transitions in living systems because of its intrinsic sensitivity (83% of the proton), large chemical shift range, and most importantly, the essentially complete lack of background interference from fluorine's near absence in biology (36, 37). $^{19}$F can be biosynthetically inserted into the side chains of tryptophan (38), tyrosine, phenylalanine (25), or via the unnatural amino acid trifluoromethyl-phenylalanine (35).

Fu et al. (33) characterized the lipoprotein receptor LR11 transmembrane domain in native *E. coli* membranes using solid-state MAS NMR. The assignments were obtained by using the $^{13}$C PARIS experiments and comparing the secondary structure in artificial membrane environments (e.g., detergent micelles, synthetic lipid bilayers) and native *E. coli* cells. Frederick et al. (39) applied DNP NMR to the yeast prion protein Sup 35, observed structural differences between purified samples and samples in cellular milieus, and concluded that the cellular environment alters Sup35 structure. The approaches described above offered good opportunities to validate and refine proteins structures in living cells.

## 2.2. Protein Interactions

Proteins perform their function by interacting with their ligands or substrates. Investigating protein interactions in cellular environment will lead to deeper understanding of molecular mechanism of protein functions.

**2.2.1. Protein–protein interactions.** Many biological functions depend on protein–protein interactions. In-cell NMR can be a powerful tool for obtaining detailed information about these interactions, but an important caveat must be kept in mind. Due to inherent low sensitivity, NMR experiments require concentrations in the tens of microns range, far above normal expression levels. Consequently, all proteins involved in a particular interaction network must be overexpressed.
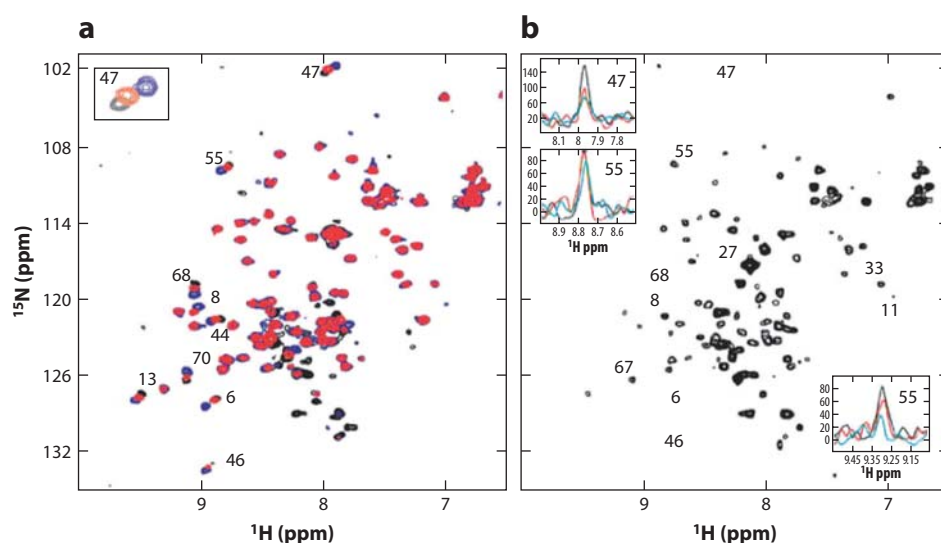
**Figure 4**

Spectra of the target protein, ubiquitin, complexed with interacting peptide, AUIM, and with interacting protein, STAM2. (*a*) Overlay of $^1$H–$^{15}$N HSQC spectra of *Escherichia coli* cells after 3 h expressing [U-$^{15}$N] ubiquitin and 0 h (*black*), 2 h (*red*), and 3 h (*blue*) expressing AUIM. Individual peaks exhibiting large shift changes are labeled with their assignments. The progression of colors in the overlaid spectra was chosen for ease of viewing. (*Inset*) Close-up of Gly47 shift changes during titration. (*b*) $^1$H–$^{15}$N HSQC spectra of *E. coli* cells after 3 h expressing [U-$^{15}$N] ubiquitin and 3 h expressing STAM2. Crosses indicate crosspeaks exhibiting extreme broadening. (*Insets*) One-dimensional traces of selected resonances exhibiting differential broadening after 3 h expressing [U-$^{15}$N] ubiquitin and 0 h (*black*), 2 h (*red*), and 3 h (*blue*) expressing STAM2. The numbers 47, 55, and 67 denote the residue numbers. Figure and caption reproduced with permission from Reference 44. Copyright 2010, Current Protocols in Protein Science Publishing Group.

Rigorous control experiments to test target protein leakage must also be performed to avoid false results (40–42).

A protein–protein interaction study with two overexpressed proteins using STINT (structural interactions using NMR spectroscopy)-NMR was reported by Shekthman and coworkers (43). To distinguish the proteins in the complex they designed a sequential expression system that enabled the target protein to be expressed in uniformly [U-$^{15}$N]-enriched medium independently under the control of an L-arabinose inducible promoter. Next, they used IPTG-induction to initiate the expression of the binding partner in unenriched medium for up to 18 h. Samples were collected at various times, and $^1$H–$^{15}$N HSQC NMR spectra of the [U-$^{15}$N] target protein were acquired. Binding was monitored in the serial in-cell spectra of the target protein as a function of the increasing concentration of the interacting proteins (**Figure 4**).

Another recent study focuses on detecting protein–protein interactions by using singular value decomposition (45), which differentiates concentration-dependent and -independent events and identifies the principal binding modes. Interaction of the prokaryotic ubiquitin-like protein (Pup) and mycobacterial proteasome ATPase (Mpa) (46) was investigated by this method. The results implicated a set of amino acids involved in a specific interaction different from previous NMR analyses but in good agreement with crystallographic data (47).

In-cell NMR experiments are routinely performed in *E. coli* by overexpressing an $^{15}$N-labeled protein (48). The application of in-cell NMR to eukaryotic cells, however, is limited by

inefficient delivery of isotope-enriched proteins. In 2009, Inomata et al. (49) reported a novel in-cell NMR method that used a cell-penetrating tag to deliver proteins into the mammalian cells. In 2013, Kubo and coworkers (50) used a pore-forming toxin, streptolysin O, to introduce enriched target proteins into mammalian cells by diffusion and used a gel-encapsulated bioreactor system for NMR studies of protein–protein interactions in living mammalian cells. The bioreactor made it possible to prolong the NMR experimental time. By using these methods, an Ile$\delta$1, Leu$\delta$1/2, and Val $\gamma$1/2 $^{13}$C (ILV) selectively enriched CAP-Gly1 domain (ILV-CG1) and a 9-kDa micro-tubule (MT)-binding domain of CLIP-170 were introduced into HeLa cells. Thus, an $^1$H–$^{13}$C band–selective optimized flip-angle short-transient heteronuclear multiple quantum coherence (SOFAST-HMQC) spectrum was acquired. The transferred cross-saturation (TCS) (51) method was employed to identify the binding interface of exogenously introduced CG1 for endogenous MTs. By comparing the HMQC spectra of ILV-CG1 obtained in cell and in vitro in the presence of purified MTs, Kubo et al. (50) determined that the intensity reductions in the in-cell TCS experiment were due to the interaction with endogenous MTs. This showed that the binding surface of an exogenously introduced protein interacting with an endogenous macromolecular complex can be identified with the TCS method.

### 2.2.2. Protein–drug interactions.

NMR spectroscopy has become an important tool for investigating protein–drug interactions in the pharmaceutical industry (52–56). The results of in vitro assays, however, might be different from those inside cells. For example, a drug might not be able to pass the cellular membrane, or it might be pumped out of cells. In addition, the drug could be metabolized or could strongly interact with other cellular components instead of the target. With these uncertainties, we cannot obtain comprehensive conclusions by merely relying on in vitro experiments. In-cell NMR enables us to examine native interactions directly. Recently, the interaction between the bacterial signal transduction protein CheY and the drug BRL-16492PA was described by Hubbard et al. (57). By comparing $^1$H–$^{15}$N HSQC spectra of the protein inside and outside of cells and comparing spectra before and after adding the drug, they found that the drug passed the bacterial membrane and interacted with target protein inside the cellular environment (**Figure 5**). A similar study of interaction between cisplatin and Atox1 was described by Arnesano et al. (58). This contribution appears to be the first direct evidence to visualize cisplatin crossing the cell membrane and interacting with the CxxC metal-binding motif of Atox1. The authors demonstrated the feasibility of in-cell NMR to monitor metallodrug–protein interactions in the native complex environment.

Xie et al. (60) developed an in-cell NMR assay for screening small-molecule interactor libraries (SMILI) for compounds capable of disrupting or enhancing specific interactions between two or more components of a biomolecular complex. To demonstrate the efficacy of SMILI-NMR in the screening of dipeptides that facilitate heterodimerization, they used a well-studied protein complex involved in cell-cycle arrest, FKBP-FRB, as a model (**Figure 6**). In fact, the dipeptides identified by SMILI-NMR possess biological activity in yeast. The in-cell nature of SMILI-NMR ensures that the screened small molecules are capable of penetrating the cell membrane and specifically engaging the target molecule(s).

Besides the target proteins, NMR signals of small drugs can also be used to study protein–drug interactions in cells. For instance, hydrolysis of antibiotics by the New Delhi metallo-$\beta$-lactamase subclass 1 (NDM-1) in *E. coli* was monitored in real time (62) (**Figure 7**). NDM-1 is one reason superbugs are resistant to most antibiotics (63). Carbapenems, such as meropenem and imipenem, once a last resort to treat the most serious bacterial infections, are hydrolyzed by NDM-1 (64). Ma et al. (62) used one-dimensional (1D) $^1$H NMR spectroscopy to monitor the hydrolytic decomposition of the carbapenem antibiotic meropenem in *E. coli* cells expressing NDM-1
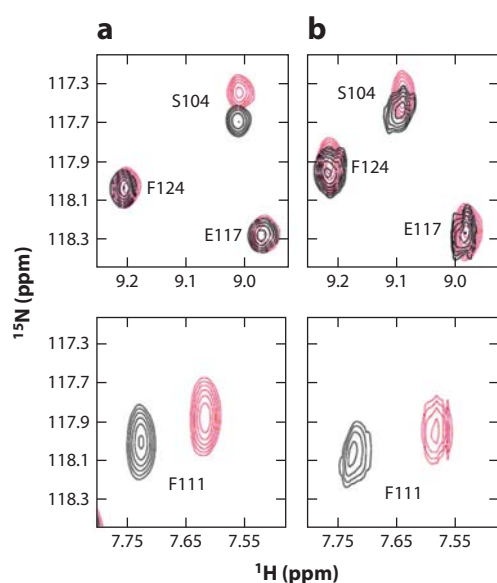
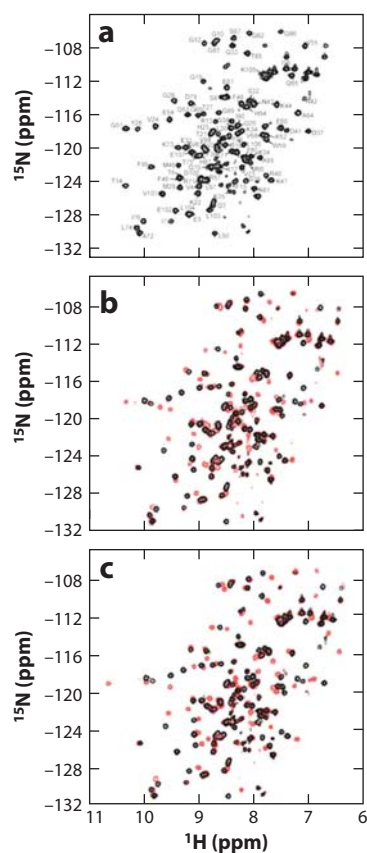**Figure 5**

Two regions of the $^{15}$N-edited HSQC spectrum of [U-$^{15}$N] CheY in the presence and absence of the drug BRL-16492PA, acquired in vitro and in cells. Spectral peaks are labeled with resonance assignments. (*a*) High-resolution in vitro HSQC spectrum of CheY in the presence of 7.4 mM MgCl$_2$ and 2 mM BRL-16492PA. This figure shows the overlay of two separate experiments: The red spectrum corresponds to the presence of BRL-16492PA, and the black spectrum corresponds to the control (no added BRL-16492PA). (*b*) HSQC spectrum of a 10% (v/v) slurry of *Escherichia Coli* cells expressing [U-$^{15}$N] CheY after isolation at 4°C and in the presence (*red spectrum*) and absence (*black spectrum*) of BRL-16492PA. The x- and y-axes denote the chemical shift of $^1$H and $^{15}$N, respectively. Figure and caption reproduced with permission from Reference 59. Copyright 2003, Molecular Microbiology Publishing Group. Abbreviation: HSQC, heteronuclear single-quantum correlation.

(**Figure 7c**). These studies show that two known NDM-1 inhibitors, L-captopril and ethylene-diaminetetraacetic acid, and a new inhibitor, spermine, inhibit the hydrolysis of meropenem in cells. This in-cell small-molecule NMR approach should be applicable to studies of protein–drug interaction in mammalian cells.

**2.2.3. Protein–DNA/RNA interactions.** Protein–DNA and protein–RNA interactions play essential roles in replication and transcription. NMR studies of protein–DNA/RNA interactions in cells are rarely reported, possibly due to their large molecular weight, which broadens resonances into the background. To the best of our knowledge, there is only one report on protein–DNA interaction. Augustus et al. (65) investigated the nonspecific association of metJ and genomic DNA in cells. Using these data, they deduced a mechanism for metJ binding to metbox sequences, which regulates methionine biosynthesis.

MetJ was uniformly [U-$^{15}$N] enriched and overexpressed in bacteria. The $^1$H–$^{15}$N HSQC spectra contained only a few weak signals in intact cells and lysed cells. Because metJ is a DNA-binding protein and is present at a substantial excess over metbox sequences in the cell, broad nonspecific interaction with DNA was postulated as the reason for the loss of NMR signals. To test this hypothesis, sonicated salmon sperm DNA was titrated into a solution of purified [U-$^{15}$N]-enriched metJ in vitro. The original sharp metJ peaks gradually broadened and ultimately disappeared with the increasing concentration of DNA, and no chemical shifts changes were observed. NMR provides an alternative method for studying protein–DNA/RNA interactions in
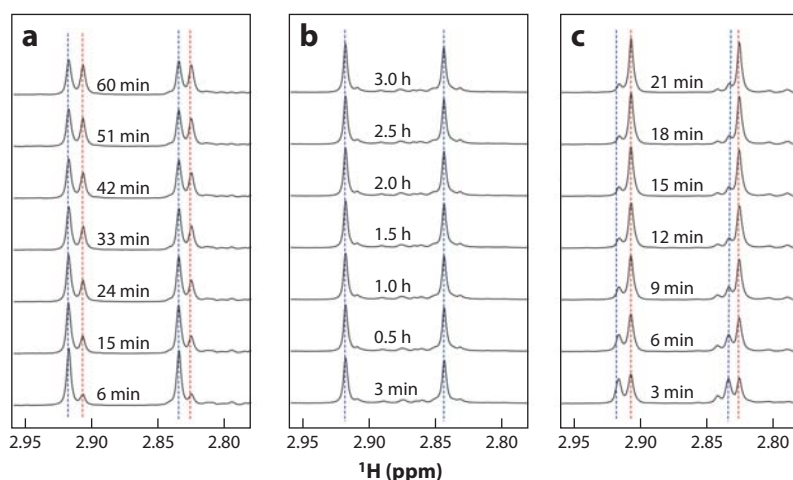
**Figure 6**

In-cell spectra of the ternary [U-$^{15}$N] FKBP–FRB–rapamycin and [U-$^{15}$N] FKBP–FRB–ascomycin complexes. (*a*) Backbone assignment of FKBP after 4-h overexpression of [U-$^{15}$N] FKBP and 4-h sequential overexpression of FRB. At typical intracellular concentrations, there is no interaction between FKBP and FRB (61). (*b*) Overlay of $^{1}$H–$^{15}$N HSQC spectra of *Escherichia coli* after 4-h overexpression of [U-$^{15}$N] FKBP and 4-h sequential overexpression of FRB in the absence (*black*) and presence (*red*) of 150 μM of rapamycin. (*c*) Overlay of $^{1}$H–$^{15}$N HSQC spectra of *E. coli* after 4-h overexpression of [U-$^{15}$N] FKBP and 4-h sequential overexpression of FRB in the absence (*black*) and presence (*red*) of 150 μM of ascomycin. Figure and caption reproduced with permission from Reference 60. Copyright 2009, Journal of Medicinal Chemistry Publishing Group. Abbreviation: HSQC, heteronuclear single-quantum correlation.

living cells, but new labeling methods and the investigation of more systems are needed to gain more information.

## 2.3. Protein Modifications

Posttranslational protein modifications endow the proteome with the ability to extend the information potential of the genetic code and rapidly reprogram protein functions in response to cellular signaling events. Errors in posttranslational modifications constitute causal agents of many human diseases. Most eukaryotic modifications denote reversible covalent additions of small chemical entities, such as phosphate, acyl, alkyl, and glycosyl groups onto subsets of modifiable amino acids (66). Common laboratory techniques to study protein phosphorylation usually rely on generic

**Figure 7**

(a) $^1$H spectra of meropenem hydrolysis in the presence of 5 nM of purified NDM-1 enzyme *Escherichia coli* cells ($OD_{600}$ = 10.0), (b) without NDM-1 plasmid, and (c) *E. coli* cells ($OD_{600}$ = 2.5) expressing NDM-1. All samples were prepared in 50 mM of sodium phosphate at pH 7.0 with 10% deuterated water. The hydrolysis of meropenem (100 μM) at different times was monitored by focusing on the $^1$H NMR signals from the nitrogen-attached methyl groups. The blue and red dashed lines denote the signals of substrate and product, respectively. Figure and caption reproduced with permission from Reference 62. Copyright 2014, Angewandte Chemie International Edition Publishing Group. Abbreviations: NDM-1, New Delhi metallo-β-lactamase subclass 1; NMR, nuclear magnetic resonance.

radionucleotide incorporation experiments, specific antibodies, or mass spectrometry; however, all of these techniques require cell fixation or cell disruption (67). In-cell NMR is ideally suited to study protein posttranslational modifications because protein resonances are highly sensitive to the chemical environments of individual residues in protein resulting from adding chemical entities. Most importantly, cellular dynamic and stepwise modifications can be measured in a nondestructive and time-resolved manner in living cells (66, 68).

**2.3.1. Protein phosphorylation.** Burz & Shekhtman (69) developed an in-cell methodology to examine the effect of posttranslational modifications on protein–protein interactions in bacterial cells by STINT-NMR. They introduced the target protein, phosphorylating interactor proteins, and kinase on separate inducible plasmids, and changes in the interaction surface of the target protein were identified. To study the phosphorylation-regulated binding of ubiquitin to STAM2 and HRS in bacteria, [U-$^{15}$N]-ubiquitin expression was induced prior to or following 3 or 4 h of STAM2 and HRS expression. The overexpression of constitutively active Src-family tyrosine kinase Fyn was induced for the final 2 h of STAM2, HRS, or STAM2-HRS expression. The spectra of ubiquitin interacting with STAM2 and HRS revealed that phosphorylation on HRS did not change the binding surface, whereas a smaller surface was involved in the interaction with phosphorylated STAM2 compared to nonphosphorylated STAM2. It was proved that the interaction surface was significantly modulated by the phosphorylation state of two STAM2 tyrosines, Y371 and Y374. This methodology enables regulation of the posttranslational modification of overexpressed proteins in bacterial cells, and the protein–protein interactions in the absence and presence of posttranslational modifications can also be studied within a cellular environment.

Compared to protein phosphorylation in bacteria, protein phosphorylation in eukaryotic cells can be realized through endogenous kinases. Bodart et al. (70) used in-cell NMR spectroscopy to examine the phosphorylation of the Tau protein in oocytes. $^{15}$N-enriched Tau was overexpressed in *E. coli*, and the purified protein was injected into *Xenopus* oocytes. A Ficoll solution was used to prolong the oocyte survival, thus allowing detection of lower protein concentrations in the oocytes. Comparing the spectrum obtained from Tau-injected oocytes to that of Tau phosphorylated in vitro indicated that PKA- but not Gsk3β-phosphorylated Tau at Ser214. The results indicate that in-cell NMR spectroscopy in *Xenopus* oocytes can identify individual phosphorylated residues and the enzyme responsible for a specific posttranslational modification.

Moreover, in-cell NMR is ideally suited for nondestructive investigations of phosphorylation events in intact cells and stepwise time-dependent modification events. Selenko et al. (71) studied the phosphorylation of substrates at adjacent sites by an endogenous kinase in oocytes using time-resolved, high-resolution NMR. The [U-$^{15}$N]-enriched substrate protein XT111–132GB1 was microinjected into *Xenopus* oocytes, and the phosphorylation activity of native CK2 on XT111-132GB1 in intact oocytes was investigated by recording NMR spectra. In accordance with in vitro experiments, signals from inside cells revealed that protein kinase CK2 phosphorylated the regulatory region of the viral SV40 large T antigen on residues Ser112 and Ser111 in a preferred order (**Figure 8**). The authors concluded that CK2 phosphorylated XT111-132GB1 via the same mechanism both in vitro and in cells, and in-cell NMR allows endogenous kinase phosphorylation to be studied in a time-resolved manner.

In addition to characterizing protein phosphorylation states, in-cell NMR is also used to investigate phosphorylation-modulated biological events. Luh et al. (73) studied the role of phosphorylation on Pin1 nonspecific interactions with the endogenous components of *Xenopus* oocytes by injecting [U-$^{15}$N]-enriched Pin1. None of the backbone amide Pin1 signals were observed in the corresponding $^{15}$N–$^{1}$H SOFAST-HMQC NMR spectrum, suggesting that most Pin1 interacted with the endogenous components of the oocytes. In subsequent experiments, the kinase PKA was used to phosphorylate Pin1 at Ser16. The phosphorylation-mimicking mutant *WWS16E* was injected into oocytes, and the resulting NMR spectrum showed all of the expected backbone amide resonances. This suggests that phosphorylation at Ser16 disrupted its nonspecific stickiness to endogenous components of the oocyte. Furthermore, the 2D SOFAST-HMQC spectrum of PKA-phosphorylated WW domain (WWS16P) in oocyte extract showed a well-dispersed and resolved spectrum, in contrast to the nonphosphorylated WW domain.

**2.3.2. Acetylation.** Selenko's group (18) derived atomic-resolution insights into the structure and dynamics of α-synuclein in mammalian cells by NMR and EPR spectroscopy. $^{15}$N-enriched α-synuclein was delivered into cultured non-neuronal A2780, HeLa cells, neuronal B65, SK-N-SH, and RCSN-3 cells by electroporation. The resulting in-cell spectra exhibited reduced signal intensities for the first 10 residues with peak positions that closely matched those of the N-terminally acetylated proteins. This observation suggested that electroporation-delivered nonacetylated α-synuclein might be N-terminally acetylated by endogenous enzymes in the cells, challenging the view that N-terminal acetylation of eukaryotic proteins was cotranslational.

**2.3.3. Oxidation.** Methionine oxidation is difficult to study because sulfoxides are not easily detected with chemical probes or antibodies. By contrast, oxidized methionines display unique NMR chemical shifts that are readily identified in 2D $^{1}$H–$^{15}$N and $^{1}$H–$^{13}$C correlation spectra. By using in-cell NMR, Selenko and coworkers (74) investigated the fate of methionine-oxidized α-synuclein, which was predicted to promote cytotoxic α-synuclein oligomers in mammalian cells.
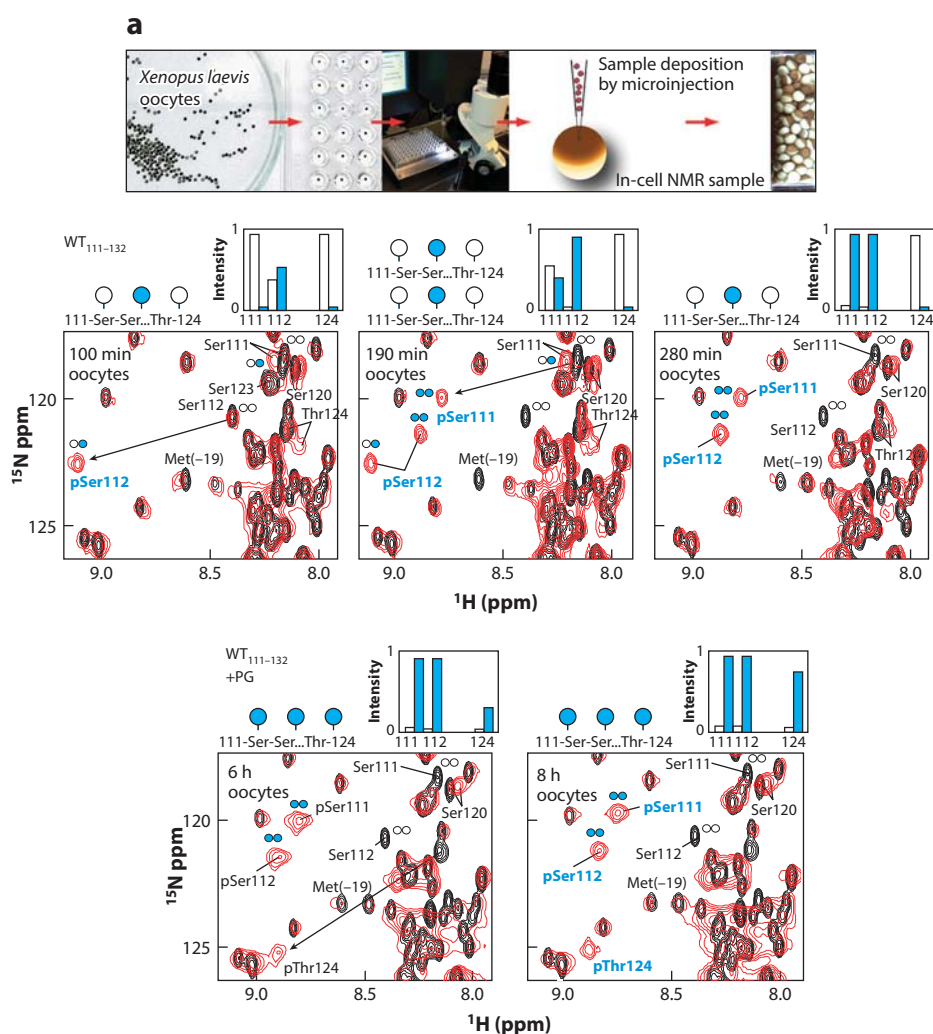
**Figure 8**

In vivo phosphorylation of XT111–132GB1 in *Xenopus laevis* oocytes. (*a*) Overview of the in-cell NMR sample preparation scheme using intact oocytes. (*b*) Time-resolved phosphorylation of XT111–132GB1 in live cells. In-cell NMR experiments of XT111–132GB1–injected oocytes show the in-cell phosphorylation of Ser112, followed by the phosphorylation of Ser111. (*c*) Progressive threonine 124 phosphorylation after PG addition to XT111–132GB1-injected oocytes. Figure and caption reproduced with permission from Reference 71. Copyright 2008, Nature Publishing Group. Abbreviations: NMR, nuclear magnetic resonance; PG, progesterone; Ser, serine; Thr, threonine; WT, wild-type.

[U-$^{15}$N]- or selective $^{15}$N-Met–enriched $\alpha$-synuclein with oxidized methionines were electroporated into A2780- and RCSN-3–cultured cells. Reduction of oxidized $\alpha$-synuclein by endogenous methionine sulfoxide reductase was studied in a time-resolved manner. The authors (74) found that the crosspeaks of Met1 and Met5 matched those of the reduced $\alpha$-synuclein, whereas Met116 and Met127 sulfoxides persisted. Furthermore, studying the [U-$^{15}$N]-enriched $\alpha$-synuclein in the lysates of mammalian cells indicated that sulfoxide N-terminal reduction of

α-synuclein proceeds in a strictly stepwise manner, with Met5 processed before Met1. The authors also studied the impact of methionine oxidation on the posttranslational modification behavior of α-synuclein. The data showed that the persistence of the C-terminal methionine sulfoxides affected the phosphorylation of Tyr125 by the tyrosine kinase Fyn but not Ser129 phosphorylation by PLK3, suggesting that oxidative damage at Met116 and Met127 modulates the phosphorylation of synuclein Y125 in mammalian cells. This work demonstrated the unique capability of in-cell NMR to characterize methionine oxidation and its biological effects in mammalian cells.

## 2.4. Protein Maturation

Impaired maturation of human superoxide dismutase 1 (SOD1) is linked to various diseases. SOD1 was transiently expressed in HEK293T cells, and [U-$^{15}$N]- or selectively $^{15}$N-cysteine–enriched SOD1 were employed to study its posttranslational maturation process in living cells by NMR. It was found that apo-SOD1 is largely unfolded and monomeric in human cells grown without zinc or copper ion supplements. Copper loading and oxidation of the Cys57–Cys146 disulfide bond is achieved in cells coexpressing SOD1 and CCS protein (**Figure 9**) (75). This study indicated that in-cell NMR represents an ideal method to monitor endogenously expressed protein maturation in human cells.

## 2.5. Protein Stability

Developing methods to measure protein stability in living cells is essential for understanding protein function under physiological conditions. NMR (76, 77), mass spectrometry (78), Raman microscopy (79), and fluorescence microscopy (80) methods have been developed to measure protein stability in living cells. Compared to other methods, NMR has the advantage that it can quantify stability at the residue level. Monteith & Pielak (76, 77) exploited NMR-detected hydrogen–deuterium (H/D) exchange of quenched cell lysates to measure individual opening free energies of GB1 in living *E. coli* cells without adding chemical denaturant or heating. Calculation of the opening free energies relied on previous work showing that the cytoplasm does not change that of amide protein exchange in unstructured peptides (81, 82). Their results (**Figure 10**) indicate that the cytoplasm of *E. coli* destabilizes GB1 in cells compared to buffer. The destabilization is caused by transient interactions between GB1 and *E. coli* proteins. Their report (76) stated that GB1 was stabilized, but further investigation revealed that the pH in cells was lower than originally thought (83); a correction was subsequently published (77).

Monteith et al. (84) also used the NMR-detected H/D exchange to quantify quinary interactions between the GB1 and cytosol of *E. coli*. They found that a surface mutation in the GB1 is ten times more destabilizing in *E. coli* than in buffer, which could be the result of quinary interactions. They demonstrated that quinary interactions modulate protein stability in cells. Smith et al. (85) developed an $^{19}$F NMR method to measure the temperature dependence of protein stability in living *E. coli*. Their results indicated that the proteins are not stabilized inside cells compared with buffer alone, consistent with previous reports.

Danielsson et al. (86) used in-cell NMR to study the thermal unfolding of a β-barrel protein SOD1$^{I35A}$ inside mammalian and bacterial cells. [U-$^{15}$N]-enriched SOD1$^{I35A}$ was overexpressed in *E. coli* and delivered into the cytosol of human ovary adenocarcinoma A2780 cells by electroporation. They acquired high-resolution in-cell HMQC spectra of SOD1$^{I35A}$ in A2780 cells and *E. coli*. The volumes of SOD1$^{I35A}$ C-terminal Q153 crosspeaks of both folded and unfolded states were used to quantify the folding free energy under different temperatures. Their results showed that SOD1$^{I35A}$ was destabilized both in *E. coli* and A2780 cells. *E. coli* decreased the transition
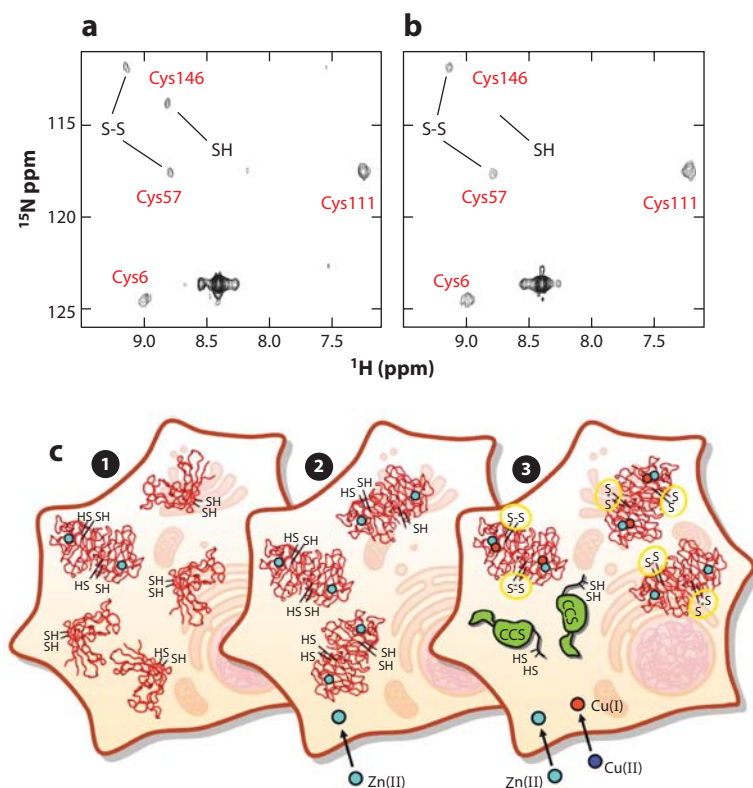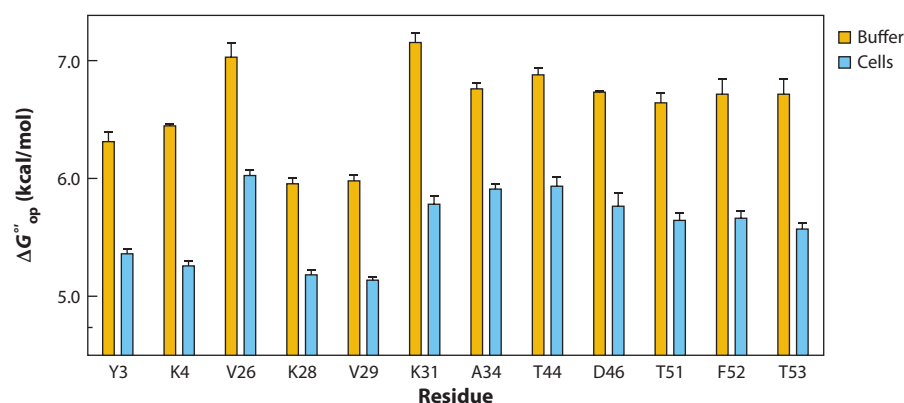
**Figure 9**

(*a,b*) $^1$H–$^{15}$N SOFAST HMQC spectra acquired on human cells coexpressing [$^{15}$N]cysteine-labeled SOD1 and CCS protein in Zn(II)-supplemented medium before (*a*) and after (*b*) incubation with Cu(II). Assigned cysteine residues are shown in red. When two species of SOD1 are present, labels indicate the cysteine redox state of each species. Unlabeled crosspeaks are cellular background signals. (*c*) Summary illustration of SOD1 maturation steps. ❶ In cells with no additional metals, SOD1 is present mainly in the monomeric partially unfolded apo form. A fraction of SOD1 binds the Zn$^{2+}$ present in the expression medium. ❷ SOD1 quantitatively binds one Zn$^{2+}$ ion per monomer and dimerizes upon addition of Zn(II) (*cyan*) to the expression medium; the cysteines involved in the intrasubunit disulfide bond are completely reduced. ❸ A fraction of SOD1 binds Cu(I) (*orange*) when Zn(II) and Cu(II) (*blue*) are added to the expression medium and CCS is coexpressed; the disulfide bond is completely formed (*yellow circles*). Figure and caption reproduced with permission from Reference 75. Copyright 2013, Nature Publishing Group. Abbreviations: Cu, copper; SOD1, superoxide dismutase 1; SOFAST-HSQC, band-selective optimized flip-angle short-transient heteronuclear single-quantum correlation; S-S, oxidized cysteines forming a disulfide bond.

temperature $T_m$ to a smaller extent than A2780 cells. Above room temperature, SOD1$^{I35A}$ was more stable in *E. coli* than in A2780 cells, whereas at lower temperature, SOD1$^{I35A}$ was more stable in A2780 cells. These data show that the cytoplasm can destabilize proteins compared to buffer.

# 3. MAGNETIC RESONANCE STUDIES OF CELL SURFACE CARBOHYDRATES

In-cell NMR is mainly used to study structures and dynamics of molecules inside cells. A different approach, on-cell NMR, has been used to study carbohydrates on the cell surface (87).

**Figure 10**

$\Delta G^{\circ\prime}_{op}$ values for WT GB1 residues in buffer and in cells. Error bars represent the standard deviation of the mean from three trials. Figure and caption reproduced with permission from Reference 77. Copyright 2015, National Academy of Sciences Publishing Group. Abbreviations: GB1, protein G B1 domain; WT, wild-type.

Carbohydrates perform essential roles, including cell–cell communication, microbial pathogenesis, autoimmune disease progression, and cancer metastasis (88). Over the last 10 years, solution and solid-state on-cell NMR methods were developed for analyzing polysaccharides.

Azurmendi et al. (89) used solution NMR to assess the structure of capsular polysaccharides (PSs) on intact cells. PSs were enriched with [U-$^{15}$N/$^{13}$C]-enriched sialic acid, thus avoiding background from other biomacromolecules, such as proteins, lipids, and nucleic acids. This is a promising approach to characterize the structural differences between PSs in cells and in vitro. Subsequently, pulse sequences based on H3-C2, H3-C1, and C1-C2 correlations were developed to characterize sialic acid resonance with high specificity (90). The sequences are also useful for studying larger sialylated glycoconjugates, including glycolipids, glycoproteins, and capsular PSs on cell surfaces.

The applicability of solution NMR depends on molecular rotational tumbling rate. Specific interactions, even transient interactions, with other cellular components will slow tumbling, resulting in broad resonances that are beyond detection. Solid-state NMR is not limited by molecular tumbling rate and therefore may be a better option for studying large-cell surface PSs (91, 92). By using the high-resolution magic-angle spinning (HR-MAS) technique, Jachymek et al. (93) demonstrated that the immunodominant O-polysaccharide on bacterial surfaces had the same structure as that in lipopolysaccharides and in isolated PSs. HR-MAS was also used to study capsular PSs, particularly sugar and capsular glycan modifications on *Campylobacter* cells (94), as well as the chemical composition and architecture of the bacterial and plant cell wall (95–99) and whole microalgae (100). In addition, evolution of the O-acetylation of the O-antigen on the outer bacteria membrane has been traced by HR-MAS (30). Such studies may promote vaccine development and contribute to drug design and discovery (101–103).

Compared to that of proteins and nucleic acids, knowledge of the structure and function of carbohydrates remains limited. The broad glycan chain diversity makes structural research difficult (104). New methods and techniques are required, especially for studying carbohydrates under physiological conditions.

## 4. MAGNETIC RESONANCE STUDIES OF RNA AND DNA

Nucleic acids are essential to all known forms of life. NMR has become an important tool in nucleic acid structure research in vitro, but many observations suggest that nucleic acid folding depends on environment. In fact, the choice of NMR in a dilute buffer cannot mimic all the factors that modulate topologies in vivo. Despite poor resolution, researchers attempting to study the in situ folding of G-quadruplex observed differences between in vitro and in-cell NMR spectra (105). Overall, the characterization of nucleic acid structure needs to be performed in as close to a native environment as possible, preferably in intact cells.

In-cell NMR strategies for nucleic acid research are similar to those for proteins: (*a*) acquiring reference spectra of nucleic acid fragments under various in vitro conditions that simulate different aspects of in-cell experiments, (*b*) characterizing physiologically relevant structures in specific buffer compositions, and (*c*) identifying the factors that define the conformation of nucleic acid in cells.

The increasing number of fingerprint NMR spectra of nucleic acid sequences in buffer paves the way for studying nucleic acids in physiologically relevant environments. Nevertheless, barriers to achieving such studies include the increased viscosity of the cellular interior compared to buffer, the transient attractive interactions that arise in the crowded cytoplasm (106), and the large size of nucleic acid fragments for in-cell NMR investigations.

In 2009, Hansel and coworkers (107) microinjected nucleic acid into *Xenopus* oocytes and recorded in-cell NMR spectra. As expected, the increased viscosity and heterogeneity of the cellular environment increase the width of resonances from in-cell samples. Despite the intensity decrease, the patterns in 2D [$^1$H-$^{13}$C]-constant time-transverse relaxation-optimized-HSQC spectra from hairpin structures are essentially identical to those from spectra acquired in vitro. During the experimental period, new signals appeared, and the original signal intensities decreased, possibly due to the degradation by nucleases. The degradation problem was a primary obstacle for in-cell nucleic acid NMR. The authors found that the window for data acquisition in cells was typically less than 6 h and that RNA was more stable than DNA with a window of 19 h (**Figure 11**). Both backbone phosphorothioate-modified nucleic acids and O2′-methylation of RNA enhanced nuclease resistance, thereby increasing the window for acquiring high-quality data in cells.

One advantage of nucleic acid over proteins and carbohydrates is the lack of cellular background in the imino region of the 1D $^1$H NMR spectrum. As imino resonances are central reporters of folding, basic structural information in cells could be obtained by selectively detecting the imino region of unenriched nucleic acid. For example, the 1D $^1$H spectrum of an unlabeled typical G-quadruplex, d[G$_3$(TTAG$_3$)$_3$T], which is relatively stable in cells, was acquired from *Xenopus* oocyte samples. The imino–proton pattern in cells was remarkably different from that in vitro, indicating that alternative conformations formed in cells (107). These differences highlight the need for in-cell studies to gain biologically relevant information.

G-quadruplex–ligand interactions were examined in *Xenopus* oocytes by Salgado et al. (108). $^1$H–$^{15}$N SOFAST-HMQC spectra of the [U–$^{15}$N/$^{13}$C]-enriched quadruplex and its complex in oocytes were recorded (**Figure 12**). The ligand was either microinjected with the quadruplex or freely diffused into oocytes from the medium, which resulted in amino signature differences, although the spectral resolution in oocytes was poor. This work demonstrates the possibility of quantifying nucleic acid–ligand interactions in living cells, but new methods are needed to improve resolution.

Besides nucleic acid degradation, the life span of cells and leakage of the introduced DNA out of cells restrict the measurement time (107, 108). It was possible to preserve *Xenopus* oocyte viability by including 20% Ficoll solution to the buffer surrounding the cells (108). To minimize
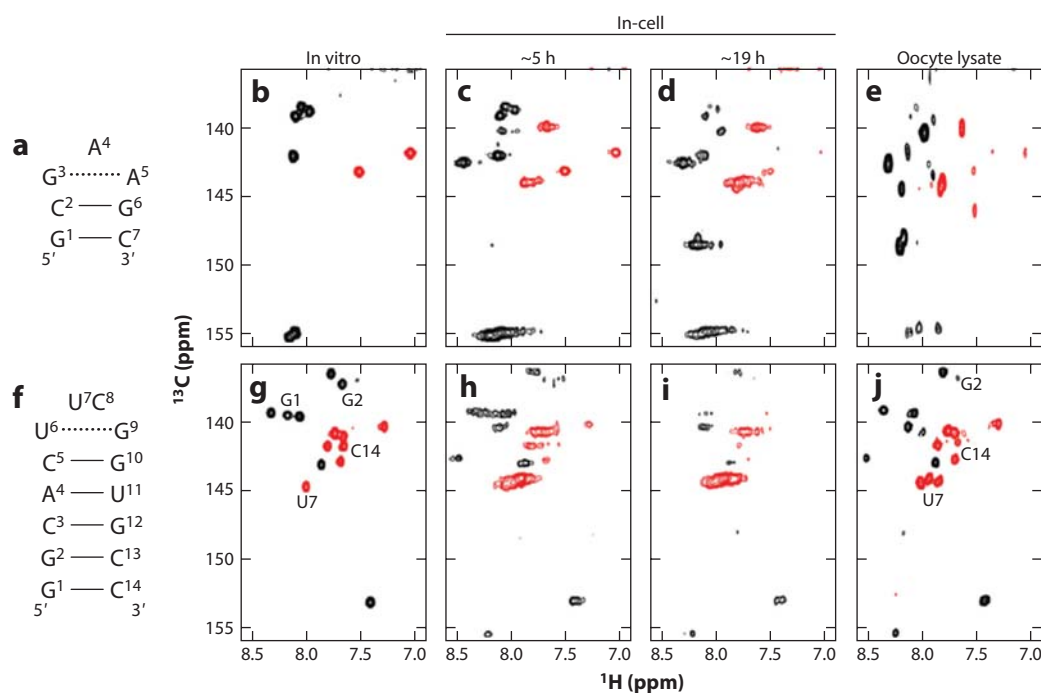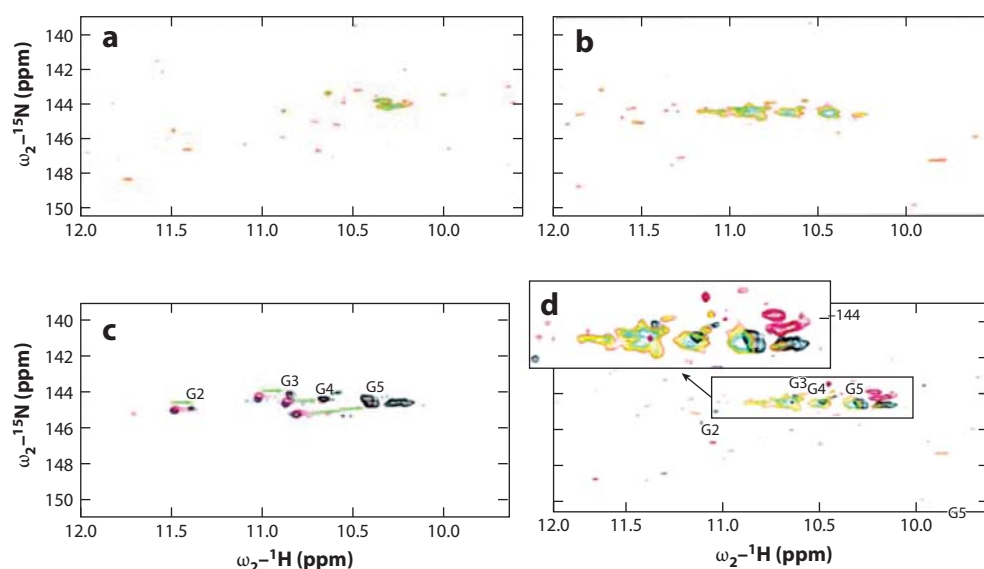
**Figure 11**

(a,f) Schematic representations of secondary structures for d(GCGAAGC) and r(GGCACUUCGGUGCC), respectively. (b–e, g–j) Aromatic regions of the two-dimensional [¹H-¹³C]-CT-TROSY spectra of ¹³C/¹⁵N-labeled d(GCGAAGC) and r(GGCACUUCGGUGCC) hairpins. (b,g) In vitro spectra of d(GCGAAGC) and r(GGCACUUCGGUGCC). (c,d) In-cell NMR spectra of d(GCGAAGC) recorded approximately 5 h and 19 h after microinjection of the *Xenopus* oocytes. (h,i) Analogous spectra to c and d for the r(GGCACUUCGGUGCC) molecule. (e,j) In vitro spectra of d(GCGAAGC) and r(GGCACUUCGGUGCC) in cleared *Xenopus* oocyte lysates. The signals in black (positive) and red (negative) correspond to purines and to pyrimidines, respectively. The difference in sign of the purine and pyrimidine peaks is due to the constant time mode of the experiment. Figure and caption reproduced with permission from Reference 107. Copyright 2009, ACS Publishing Group. Abbreviations: HQSC, heteronuclear single-quantum correlation; NMR, nuclear magnetic resonance.

damage to the cells, experiments should be carried out at ∼16°C, which also improves the quality of the imino signals. These conditions increased the available acquisition period to longer than 48 h.

Although the low sensitivity of NMR and high cellular background signals can be partially overcome by introducing large quantities of exogenous DNA (107), the inhomogenous nature of the intracellular environment also limits the application of in-cell NMR spectroscopy for nucleic acid. The maximum concentration of quadruplex DNA was 250 μM; higher concentrations caused cell death. Approximately 93% of the introduced DNA spontaneously concentrated in the nucleus, indicating the intracellular source of the NMR signals (111). ¹⁹F NMR might also be useful for improving the sensitivity. Remarkably, incorporation of fluorine-modified nucleobases, either by chemical or enzymatic synthesis, has been widely exploited for in vitro studies (112–114). The use of site-specific labeled samples will also likely improve the resolution.

Synthetically prepared nucleic acid contained some small-molecule impurities that were lethal to the oocytes. These impurities can be removed by butanol precipitation prior to injection. However, butanol precipitation washed out not only various kinds of toxic contaminants but also

**Figure 12**

Probing ligand interactions with d(TG$_4$T)$_4$ using $^1$H–$^{15}$N SOFAST-HMQC in vitro and in cells. (*a*) Ligand incubated and freely diffused from the NMR tube buffer into the interior of *Xenopus* oocytes, previously microinjected with d(TG$_4$T)$_4$. (*b*) The in-cell spectrum that resulted from the incubation of a 2.5 molar ratio of ligand 360A with d(TG$_4$T)4 for a period of 4 h (at room temperature) prior to comicroinjection in ~200 *Xenopus* oocytes. (*c*) Titration experiments in vitro without ligand (*blue*) and after incubation with 1 (*red*) and 2.5 (*black*) molar ratios of ligand to d(TG$_4$T)$_4$. (*d*) Spectra from *a* and *b* overlaid with the black spectrum of *c*. Spectra were acquired at 16°C. The spectra show important differences in the organization of the d(TG$_4$T)$_4$ tetrads after ligand binding in vitro compared to the changes observed in cells. Spectra were analyzed taking into account peak assignments described previously (109, 110) together with in vitro $^1$H–$^{15}$N HSQC titration of d(TG$_4$T)$_4$ with 360A. Figure and caption reproduced with permission from Reference 108. Copyright 2015, Royal Society of Chemistry Publishing Group. Abbreviations: NMR, nuclear magnetic resonance; SOFAST-HSQC, band-selective optimized flip-angle short-transient heteronuclear single-quantum correlation.

the ions from the G-quadruplex. Accordingly, the precipitated samples should be dissolved in buffer and reannealed before injection (107).

Investigation of nucleic acids under physiological conditions has been implemented only in oocytes. Studies in other types of mammalian cells and even in cell culture models of disease represent future research directions. To achieve the goal, clever delivery methods are needed (49, 115). NMR spectroscopy is distinctively suited to characterizing biomolecular dynamics because it can provide a comprehensive description of internal motions at various time scales (116). Hence, the next promising application of in-cell NMR involves the analysis of physiologically relevant nucleic acid dynamics.

EPR techniques such as double electron–electron resonance (DEER) spectroscopy have also been used to measure long-range distances (2–7 nm) in nucleic acid (117–119). Due to its high sensitivity, EPR could be efficiently used in living cells (120). Igarashi et al. (121) used the DEER method to determine the RNA and DNA structures in *Xenopus* oocytes. The ultimate goal of defining the relationships between nucleic acid function and the conformational fluctuations that accompany biological activity in living systems will be achieved by combining magnetic resonance methods with other in situ techniques.

## 5. HYPERPOLARIZATION TO BOOST SENSITIVITY

Owing to the insensitivity of NMR spectroscopy and the low concentration of endogenous biomacromolecules, hyperpolarization (122) holds the promise to dramatically improve the sensitivity of in-cell studies. It may even prove possible to detect endogenous protein resonances.

Spin-exchange optical pumping (SEOP) is a typical hyperpolarization method (123, 124). Hyperpolarized $^{129}$Xe via SEOP is the most widely used technique. The $^{129}$Xe chemical shift is sensitive to environment due to its extraordinarily wide range, and $^{129}$Xe also possesses favorable relaxation characteristics (125, 126). In 2000, hyperpolarized $^{129}$Xe gas was first used to detect hemoglobin in red blood cells (127). Subsequently, hyperpolarized $^{129}$Xe NMR spectra were recorded in various living cells (128). In addition to direct dissolution, $^{129}$Xe was incorporated into nonpolar cryptophanes as a biosensor to detect biomacromolecules at low concentration (129). In this sensor, $^{129}$Xe occupied the hydrophobic cavity, and interactions could be monitored by $^{129}$Xe NMR signal change upon binding with target proteins. A variety of sensors were developed to detect cancer biomarkers (130–132) and peptide–antigen interactions (133). Recently, Boutin et al. (128) used transferrin with $^{129}$Xe cryptophanes to identify transferrin receptors on the surface of K562 cells by observing the chemical shift change on binding. An antibody-based CD14-specific biosensor was developed for $^{129}$Xe magnetic resonance imaging of cells at nanomolar concentrations (134). In addition to cryptophanes, viral capsids were employed to carry $^{129}$Xe and recognize the epidermal growth factor receptor with high specificity in living cells (135).

In summary, hyperpolarized NMR improves endogenous protein detection and function analysis in living cells. In addition to SEOP, hyperpolarization methods may vastly extend the utilization of NMR for studying living cells, including parahydrogen-induced polarization (136, 137) and DNP (138, 139), which polarize the nucleus, including $^{13}$C, $^{1}$H, $^{15}$N, and $^{19}$F in proteins and nucleic acids. However, many aspects of these methods still urgently need improvement, including amelioration of the extreme hyperpolarization conditions and minimization of polarization losses in cells.

## 6. CONCLUSIONS AND PERSPECTIVES

Although significant advancements in in-cell NMR have been achieved, there remains much for us to speculate about the future. From the viewpoint of fundamental work, the research focus will be on understanding and manipulating the ubiquitous transient interactions in cells, quantifying specific protein–protein interactions in cells, and measuring enzyme kinetics and various posttranslational modifications mediated by protein function. The protein structure determination will be more significant for multidomain proteins and intrinsically disordered proteins, whose structure might be more prone to influence by the cellular environment. Most importantly, studies of macromolecules at near physiological concentrations (nanomolar to micromolar) in eukaryotic cells, especially in the cell culture model of diseases, will become important because of their potential medical relevance. Protein dynamics, which correlates with protein function, is well studied in dilute solution, but how cellular environment affects protein dynamics at various time scales is not well documented (140, 141). In terms of techniques, the development of hyperpolarization methods and instruments suitable for in-cell NMR and selective order-of-magnitude enhancements of target-molecular NMR sensitivity will broaden the in-cell NMR applications. This makes in-cell NMR an attractive approach for assessing biomolecular structure, function, and dynamics at atomic resolution in living cells.

## DISCLOSURE STATEMENT

## ACKNOWLEDGMENTS

## LITERATURE CITED

1. Zimmerman SB, Trach SO. 1991. Estimation of macromolecule concentrations and excluded volume effects for the cytoplasm of *Escherichia coli*. *J. Mol. Biol.* 222:599–620
2. Ellis RJ. 2001. Macromolecular crowding: obvious but underappreciated. *Trends Biochem. Sci.* 26:597–604
3. Eakin RT, Morgan LO, Gregg CT, Matwiyoff NA. 1972. Carbon-13 nuclear magnetic resonance spectroscopy of living cells and their metabolism of a specifically labeled $^{13}C$ substrate. *FEBS Lett.* 28:259–64
4. London RE, Gregg CT, Matwiyoff NA. 1975. Nuclear magnetic resonance of rotational mobility of mouse hemoglobin labeled with (2-$^{13}C$) histidine. *Science* 188:266–68
5. Llinas M, Wüthrich K, Schwotzer W, von Philipsborn W. 1975. $^{15}N$ nuclear magnetic resonance of living cells. *Nature* 257:817–18
6. Daniels A, Williams RJ, Wright PE. 1976. Nuclear magnetic resonance studies of the adrenal gland and some other organs. *Nature* 261:321–23
7. Li C, Charlton LM, Lakkavaram A, Seagle C, Wang G, et al. 2008. Differential dynamical effects of macromolecular crowding on an intrinsically disordered protein and a globular protein: implications for in-cell NMR spectroscopy. *J. Am. Chem. Soc.* 130:6310–11
8. Theillet FX, Binolfi A, Frembgen-Kesner T, Hingorani K, Sarkar M, et al. 2014. Physicochemical properties of cells and their effects on intrinsically disordered proteins (IDPs). *Chem. Rev.* 114:6661–714
9. Brindle KM, Williams S-P, Boulton M. 1989. $^{19}F$ NMR detection of a fluorine-labelled enzyme in vivo. *FEBS Lett.* 255:121–24
10. Serber Z, Dötsch V. 2001. In-cell NMR spectroscopy. *Biochemistry* 40:14317–23
11. Dedmon MM, Petel CN, Young GB, Pielak GJ. 2002. FlgM gains structure in living cells. *PNAS* 99:12681–84
12. Sakakibara D, Sasaki A, Ikeya T, Hamatsu J, Hanashima T, et al. 2009. Protein structure determination in living cells by in-cell NMR spectroscopy. *Nature* 458:102–5
13. Ikeya T, Sasaki A, Sakakibara D, Shigemitsu Y, Hamatsu J, et al. 2010. NMR protein structure determination in living *E. coli* cells using nonlinear sampling. *Nat. Protoc.* 5:1051–60
14. Rovnyak D, Frueh DP, Sastry M, Sun ZYJ, Stern AS, et al. 2004. Accelerated acquisition of high resolution triple-resonance spectra using non-uniform sampling and maximum entropy reconstruction. *J. Magn. Reson.* 170:15–21
15. Schmeider P, Stern AS, Wagner G, Hoch JC. 1994. Improved resolution in triple-resonance spectra by nonlinear sampling in the constant-time domain. *J. Biomol. NMR* 4:483–90
16. Anfinsen CB. 1973. Principles that govern the folding of protein chains. *Science* 181:223–30
17. Richards FM. 1977. Areas, volumes, packing and protein structure. *Annu. Rev. Biophys. Bioeng.* 6:151–76
18. Theillet F-X, Binolfi A, Bekei B, Martorana A, Rose HM, et al. 2016. Structural disorder of monomeric α-synuclein persists in mammalian cells. *Nature* 530:45–50
19. Song L, Larion M, Chamoun J, Bonora M, Fajer PG. 2010. Distance and dynamics determination by W-band DEER and W-band ST-EPR. *Eur. Biophys. J.* 39:711–19
20. Martorana A, Bellapadrona G, Feintuch A, Di Gregorio E, Aime S, et al. 2014. Probing protein conformation in cells by EPR distance measurements using $Gd^{3+}$ spin labeling. *J. Am. Chem. Soc.* 136:13458–65
21. Ye YS, Liu XL, Xu GH, Liu ML, Li CG. 2015. Direct observation of $Ca^{2+}$-induced calmodulin conformational transitions in intact *Xenopus laevis* oocytes by F-19 NMR spectroscopy. *Angew. Chem. Int. Ed.* 54:5328–30
22. Pan BB, Yang F, Ye YS, Wu Q, Li CG, et al. 2016. 3D structure determination of a protein in living cells using paramagnetic NMR spectroscopy. *Chem. Commun.* 52:10237–40

23. Müntener T, Haussinger D, Selenko P, Theillet F-X. 2016. In-cell protein structures from 2D NMR experiments. *J. Phys. Chem. Lett.* 7:2821–25

24. Hikone Y, Hirai G, Mishima M, Inomata K, Ikeya T, et al. 2016. A new carbamidemethyl-linked lanthanoid chelating tag for PCS NMR spectroscopy of proteins in living HeLa cells. *J. Biomol. NMR* 66:99

25. Xu G, Ye Y, Liu X, Cao S, Wu Q, et al. 2014. Strategies for protein NMR in *Escherichia coli. Biochemistry* 53:1971–81

26. Ye Y, Liu X, Chen Y, Xu G, Wu Q, et al. 2015. Labeling strategy and signal broadening mechanism of protein NMR spectroscopy in *Xenopus laevis* oocytes. *Chem. Eur. J.* 21:8686–90

27. Kern T, Giffard M, Hediger S, Amoroso A, Giustini C, et al. 2010. Dynamics characterization of fully hydrated bacterial cell walls by solid-state NMR: evidence for cooperative binding of metal ions. *J. Am. Chem. Soc.* 132:10911–19

28. Renault M, Tommassen-van Boxtel R, Bos MP, Post JA, Tommassen J, et al. 2012. Cellular solid-state nuclear magnetic resonance spectroscopy. *PNAS* 109:4863–68

29. Takahashi H, Ayala I, Bardet M, De Paepe G, Simorre JP, et al. 2013. Solid-state NMR on bacterial cells: selective cell wall signal enhancement and resolution improvement using dynamic nuclear polarization. *J. Am. Chem. Soc.* 135:5105–10

30. Zandomeneghi G, Ilg K, Aebi M, Meier BH. 2012. On-cell MAS NMR: physiological clues from living cells. *J. Am. Chem. Soc.* 134:17513–19

31. Barnes AB, Corzilius B, Mak-Jurkauskas ML, Andreas LB, Bajaj VS, et al. 2010. Resolution and polarization distribution in cryogenic DNP/MAS experiments. *Phys. Chem. Chem. Phys.* 12:5861–67

32. Yamamoto K, Caporini MA, Im SC, Waskell L, Ramamoorthy A. 2015. Cellular solid-state NMR investigation of a membrane protein using dynamic nuclear polarization. *Biochim. Biophys. Acta Biomembr.* 1848:342–49

33. Fu R, Wang X, Li C, Santiago-Miranda AN, Pielak GJ, et al. 2011. In situ structural characterization of a recombinant protein in native *Escherichia coli* membranes with solid-state magic-angle-spinning NMR. *J. Am. Chem. Soc.* 133:12370–73

34. Vogel EP, Curtis-Fisk J, Young KM, Weliky DP. 2011. Solid-state nuclear magnetic resonance (NMR) spectroscopy of human immunodeficiency virus gp41 protein that includes the fusion peptide: NMR detection of recombinant Fgp41 in inclusion bodies in whole bacterial cells and structural characterization of purified and membrane-associated Fgp41. *Biochemistry* 50:10013–26

35. Shi P, Li D, ChenH Xiong Y, Wang Y, et al. 2012. In situ $^{19}$F NMR studies of an *E. coli* membrane protein. *Protein Sci.* 21:596–600

36. Harper DB, O'Hagan D. 1994. The fluorinated natural products. *Nat. Prod. Rep.* 11:123–33

37. O'Hagan D, Harper DB. 1999. Fluorine-containing natural products. *J. Fluorine Chem.* 100:127–33

38. Crowley PB, Kyne C, Monteith WB. 2012. Simple and inexpensive incorporation of $^{19}$F-tryptophan for protein NMR spectroscopy. *Chem. Commun.* 48:10681–83

39. Frederick KK, Michaelis VK, Corzilius B, Ong TC, Jacavone AC, et al. 2015. Sensitivity-enhanced NMR reveals alterations in protein structure by cellular milieus. *Cell* 163:620–28

40. Pielak GJ. 2007. Retraction. *Biochemistry* 46:8206

41. Barnes CO, Pielak GJ. 2011. In-cell protein NMR and protein leakage. *Proteins* 79:347–51

42. Wang Q, Zhuravleva A, Gierasch LM. 2011. Exploring weak, transient protein–protein interactions in crowded in vivo environments by in-cell nuclear magnetic resonance spectroscopy. *Biochemistry* 50:9225–36

43. Burz DS, Dutta K, Cowburn D, Shekhtman A. 2006. Mapping structural interactions using in-cell NMR spectroscopy (STINT-NMR). *Nat. Methods* 3:91–93

44. Burz DS, Shekhtman A. 2010. The STINT-NMR method for studying in-cell protein-protein interactions. *Curr. Protoc. Protein Sci.* 61:17.11

45. Majumder S, DeMott CM, Burz DS, Shekhtman A. 2014. Using singular value decomposition to characterize protein–protein interactions by in-cell NMR spectroscopy. *ChemBioChem* 15:929–33

46. Striebel F, Imkamp F, Özcelik D, Weber-Ban E. 2014. Pupylation as a signal for proteasomal degradation in bacteria. *Biochim. Biophys. Acta Mol. Cell. Res.* 1843:103–13

47. Maldonado AY, Burz DS, Reverdatto S, Shekhtman A. 2013. Fate of Pup inside the Mycobacterium proteasome studied by in-cell NMR. *PLOS ONE* 8:e74576

48. Serber Z, Keatinge-Clay AT, Ledwidge R, Kelly AE, Miller SM, et al. 2001. High-resolution macromolecular NMR spectroscopy inside living cells. *J. Am. Chem. Soc.* 123:2446–47

49. Inomata K, Ohno A, Tochio H, Isogai S, Tenno T, et al. 2009. High-resolution multi-dimensional NMR spectroscopy of proteins in human cells. *Nature* 458:106–9

50. Kubo S, Nishida N, Udagawa Y, Takarada O, Ogino S, et al. 2013. A gel-encapsulated bioreactor system for NMR studies of protein-protein interactions in living mammalian cells. *Angew. Chem. Int. Ed.* 52:1208–11

51. Shimada I, Ueda T, Matsumoto M, Sakakura M, Osawa M, et al. 2009. Cross-saturation and transferred cross-saturation experiments. *Prog. Nucl. Magn. Reson. Spectrosc.* 54:123–40

52. Fesik SW. 1993. NMR structure-based drug design. *J. Biomol. NMR* 3:261–69

53. Mayer M, Meyer B. 2001. Group epitope mapping by saturation transfer difference NMR to identify segments of a ligand in direct contact with a protein receptor. *J. Am. Chem. Soc.* 123:6108–17

54. Mayer M, Meyer B. 2000. Mapping the active site of angiotensin-converting enzyme by transferred NOE spectroscopy. *J. Med. Chem.* 43:2093–99

55. Pellecchia M, Meininger D, Dong Q, Chang E, Jack R, et al. 2002. NMR-based structural characterization of large protein-ligand interactions. *J. Biomol. NMR* 22:165–73

56. Claasen B, Axmann M, Meinecke R, Meyer B. 2005. Direct observation of ligand binding to membrane proteins in living cells by a saturation transfer double difference (STDD) NMR spectroscopy method shows a significantly higher affinity of integrin αIIbβ3 in native platelets than in liposomes. *J. Am. Chem. Soc.* 127:916–19

57. Hubbard JA, MacLachlan LK, King GW, Jones JJ, Fosberry AP. 2003. Nuclear magnetic resonance spectroscopy reveals the functional state of the signalling protein CheY in vivo in *Escherichia coli. Mol. Microbiol.* 49:1191–200

58. Arnesano F, Banci L, Bertini I, Felli IC, Losacco M, et al. 2011. Probing the interaction of cisplatin with the human copper chaperone Atox1 by solution and in-cell NMR spectroscopy. *J. Am. Chem. Soc.* 133:18361–69

59. Hubbard JA, MacLachlan LK, King GW, Jones JJ, Fosberry AP. 2003. Nuclear magnetic resonance spectroscopy reveals the functional state of the signalling protein CheY *in vivo* in *Escherichia coli. Mol. Microbiol.* 49:1191–200

60. Xie J, Thapa R, Reverdatto S, Burz DS, Shekhtman A. 2009. Screening of small molecule interactor library by using in-cell NMR spectroscopy (SMILI-NMR). *J. Med. Chem.* 52:3516–22

61. Banaszynski LA, Liu CW, Wandless TJ. 2005. Characterization of the FKBP rapamycin FRB ternary complex. *J. Am. Chem. Soc.* 127:4715–21

62. Ma J, McLeod S, MacCormack K, Sriram S, Gao N, Breeze AL, Hu J. 2014. Real-time monitoring of New Delhi metallo-β-lactamase activity in living bacterial cells by $^1$H NMR spectroscopy. *Angew. Chem. Int. Ed.* 53(8):2130–33

63. Guo Y, Wang J, Niu G, Shui W, Sun Y, et al. 2011. A structural view of the antibiotic degradation enzyme NDM-1 from a superbug. *Protein Cell* 2:384–94

64. Patel G, Bonomo RA. 2013. "Stormy waters ahead": global emergence of carbapenemases. *Front. Microbiol.* 4:65–76

65. Augustus AM, Reardon PN, Spicer LD. 2009. MetJ repressor interactions with DNA probed by in-cell NMR. *PNAS* 106:5065–69

66. Theillet F-X, Smet-Nocca C, Liokatis S, Thongwichian R, Kosten J, et al. 2012. Cell signaling, post-translational protein modifications and NMR spectroscopy. *J. Biomol. NMR* 54:217–36

67. Young NL, Plazas-Mayorca MD, Garcia BA. 2010. Systems-wide proteomic characterization of combinatorial post-translational modification patterns. *Expert Rev. Proteom.* 7:79–92

68. Liokatis S, Dose A, Schwarzer D, Selenko P. 2010. Simultaneous detection of protein phosphorylation and acetylation by high-resolution NMR spectroscopy. *J. Am. Chem. Soc.* 132:14704–5

69. Burz DS, Shekhtman A. 2008. In-cell biochemistry using NMR spectroscopy. *PLOS ONE* 3:e2571

70. Bodart JF, Wieruszeski JM, Amniai L, Leroy A, Landrieu I, et al. 2008. NMR observation of Tau in *Xenopus* oocytes. *J. Magn. Reson.* 192:252–57

71. Selenko P, Frueh DP, Elsaesser SJ, Haas W, Gygi SP, et al. 2008. In situ observation of protein phosphorylation by high-resolution NMR spectroscopy. *Nat. Struct. Mol. Biol.* 15:321–29

72. Naganuma M, Sekine S, Chong YE, Guo M, Yang XL, et al. 2014. The selective tRNA aminoacylation mechanism based on a single GU pair. *Nature* 510:507–11

73. Luh LM, Hänsel R, Löhr F, Kirchner DK, Krauskopf K, et al. 2013. Molecular crowding drives active Pin1 into nonspecific complexes with endogenous proteins prior to substrate recognition. *J. Am. Chem. Soc.* 135:13796–803

74. Binolfi A, Limatola A, Verzini S, Kosten J, Theillet F-X, et al. 2016. Intracellular repair of oxidation-damaged α-synuclein fails to target C-terminal modification sites. *Nat. Commun.* 7:10251

75. Banci L, Barbieri L, Bertini I, Luchinat E, Secci E, et al. 2013. Atomic-resolution monitoring of protein maturation in live human cells by NMR. *Nat. Chem. Biol.* 9:297–99

76. Monteith WB, Pielak GJ. 2014. Residue level quantification of protein stability in living cells. *PNAS* 111:11335–40

77. Monteith WB, Pielak GJ. 2015. Correction for Monteith and Pielak: residue level quantification of protein stability in living cells. *PNAS* 112:E7031

78. Ghaemmaghami S, Oas TG. 2001. Quantitative protein stability measurements in vivo. *Nat. Struct. Biol.* 8:879–82

79. Wei L, Yu Y, Shen YH, Wang MC, Min W. 2013. Vibrational imaging of newly synthesized proteins in live cells by stimulated Raman scattering microscopy. *PNAS* 110:11226–31

80. Ebbinghaus S, Dhar A, McDonald JD, Gruebele M. 2010. Protein folding stability and dynamics imaged in a living cell. *Nat. Methods* 7:319–23

81. Smith AE, Sarkar M, Young GB, Pielak GJ. 2013. Amide proton exchange of a dynamic loop in cell extracts. *Protein Sci.* 2:1313–19

82. Smith AE, Zhou Z, Pielak GJ. 2015. Hydrogen exchange of disordered proteins in *Escherichia coli*. *Protein Sci.* 24:706–13

83. Cohen RD, Guseman AJ, Pielak GJ. 2015. Intracellular pH modulates quinary structure. *Protein Sci.* 24:1748–55

84. Monteith WB, Cohen RD, Smith AE, Guzman-Cisneros E, Pielak GJ. 2015. Quinary structure modulates protein stability in cells. *PNAS* 112:1739–42

85. Smith AE, Zhou LZ, Gorensek AH, Senske M, Pielak GJ. 2016. In-cell thermodynamics and a new role for protein surfaces. *PNAS* 113:1725–30

86. Danielsson J, Mu X, Lang L, Wang H, Binolfi A, et al. 2015. Thermodynamics of protein destabilization in live cells. *PNAS* 112:12402–7

87. Freedberg DI, Selenko P. 2014. Live Cell NMR. *Annu. Rev. Biophys.* 43:171–92

88. Dwek RA. 1996. Glycobiology: toward understanding the function of sugars. *Chem. Rev.* 96:683–720

89. Azurmendi HF, Vionnet J, Wrightson L, Trinh LB, Shiloach J, et al. 2007. Extracellular structure of polysialic acid explored by on cell solution NMR. *PNAS* 104:11557–61

90. Barb AW, Freedberg DI, Battistel MD, Prestegard JH. 2011. NMR detection and characterization of sialylated glycoproteins and cell surface polysaccharides. *J. Biomol. NMR* 51:163–71

91. Reckel S, Lopez JJ, Löhr F, Glaubitz C, Dötsch V. 2012. In-cell solid-state NMR as a tool to study proteins in large complexes. *ChemBioChem* 13:534–37

92. Warnet XL, Arnold AA, Marcotte I, Warschawski DE. 2015. In-cell solid-state NMR: an emerging technique for the study of biological membranes. *Biophys. J.* 109:2461–66

93. Jachymek W, Niedziela T, Petersson C, Lugowski C, Czaja J, et al. 1999. Structures of the O-specific polysaccharides from *Yokenella regensburgei* (*Koserella trabulsii*) strains PCM 2476, 2477, 2478, and 2494: high-resolution magic-angle spinning NMR investigation of the O-specific polysaccharides in native lipopolysaccharides and directly on the surface of living bacteria. *Biochemistry* 38:11788–95

94. Szymanski CM, Michael FS, Jarrell HC, Li J, Gilber M, et al. 2003. Detection of conserved N-linked glycans and phase-variable lipooligosaccharides and capsules from *Campylobacter* cells by mass spectrometry and high resolution magic angle spinning NMR spectroscopy. *J. Biol. Chem.* 278:24509–20

95. Rice DM, Romaniuk AH, Cegelski L. 2015. Frequency-selective REDOR and spin-diffusion relays in uniformly labeled whole cells. *Solid State Nucl. Magn. Reson.* 72:132–39

96. Romaniuk JAH, Cegelski L. 2015. Bacterial cell wall composition and the influence of antibiotics by cell-wall and whole-cell NMR. *Philos. Trans. R. Soc. B* 370:20150024

97. Nygaard R, Romaniuk JAH, Rice DM, Cegelski L. 2015. Spectral snapshots of bacterial cell-wall composition and the influence of antibiotics by whole-cell NMR. *Biophys. J.* 108:1380–89

98. Cegelski L, O'Connor RD, Stueber D, Singh M, Poliks B, et al. 2010. Plant cell-wall cross-links by REDOR NMR spectroscopy. *J. Am. Chem. Soc.* 132:16052–57

99. Cegelski L, Steuber D, Mehta AK, Kulp DW, Axelsen PH, et al. 2006. Conformational and quantitative characterization of oritavancin-peptodoglycan complexes in whole cells of *Staphylococcus aureus* by *in vivo* $^{13}$C and $^{15}$N labelling. *J. Mol. Biol.* 357:1253–62

100. Arnold AA, Genard B, Zito F, Tremblay R, Warschawski DE, et al. 2015. Identification of lipid and saccharide constituents of whole microalgal cells by $^{13}$C solid-state NMR. *Biochim. Biophys. Acta Biomembr.* 1848:369–77

101. Kim SJ, Cegelski L, Preobrazhenskaya M, Schaefer J. 2006. Structures of *Staphylococcus aureus* cell-wall complexes with vancomycin, eremomycin, and chloroeremomycin derivatives by $^{13}$C$\{^{19}$F$\}$ and $^{15}$N$\{^{19}$F$\}$ rotational-echo double resonance. *Biochemistry* 45:5235–50

102. Toke O, Cegelski L, Schaefer J. 2006. Peptide antibiotics in action: investigation of polypeptide chains in insoluble environments by rotational-echo double resonance. *Biochim. Biophys. Acta Biomembr.* 1758:1314–29

103. Cegelski L. 2013. REDOR NMR for drug discovery. *Bioorg. Med. Chem. Lett.* 23:5767–75

104. Battistel MD, Azurmendi HF, Yu B, Freedberg DI. 2014. NMR of glycans: shedding new light on old problems. *Prog. Nucl. Magn. Reson. Spectrosc.* 79:48–68

105. Hänsel R, Löhr F, Trantirek L, Dötsch V. 2013. High-resolution insight into G-overhang architecture. *J. Am. Chem. Soc.* 135:2816–24

106. Sarkar M, Li C, Pielak GJ. 2013. Soft interactions and crowding. *Biophy. Rev.* 5:187–94

107. Hänsel R, Foldynova-Trantirkova S, Löhr F, Buck J, Bongartz E, et al. 2009. Evaluation of parameters critical for observing nucleic acids inside living *Xenopus laevis* oocytes by in-cell NMR spectroscopy. *J. Am. Chem. Soc.* 31:15761–68

108. Salgado GF, Cazenave C, Kerkour A, Mergny JL. 2015. G-quadruplex DNA and ligand interaction in living cells using NMR spectroscopy. *Chem. Sci.* 6:3314–20

109. Sket P, Plavec J. 2010. Tetramolecular DNA quadruplexes in solution: insights into structural diversity and cation movement. *J. Am. Chem. Soc.* 32:12724–32

110. Gai W, Yang QF, Xiang JF, Jiang W, Li Q, et al. 2013. A dual-site simultaneous binding mode in the interaction between parallel-stranded G-quadruplex [d(TGGGGT)]$_4$ and cyanine dye 2,2′-diethyl-9-methyl-selenacarbocyanine bromide. *Nucleic Acids Res.* 41:2709–22

111. Hänsel R, Foldynova-Trantirkova S, Dötsch V, Trantirek L. 2013. Investigation of quadruplex structure under physiological conditions using in-cell NMR. In *Quadruplex Nucleic Acids*, ed. JB Chaires, D Graves, pp. 47–65. Berlin: Springer

112. Arnold JRP, Fisher J. 2000. Structural equilibria in RNA as revealed by $^{19}$NMR. *J. Biomol. Struct. Dyn.* 17:843–56

113. Hammann C, Norman DG, Lilley DMJ. 2001. Dissection of the ion-induced folding of the hammerhead ribozyme using $^{19}$F NMR. *PNAS* 98:5503–8

114. Olejniczak M, Gdaniec Z, Fischer A, Grabarkiewicz T, Bielecki L, et al. 2002. The bulge region of HIV-1 TAR RNA binds metal ions in solution. *Nucleic Acids Res.* 30:4241–49

115. Ogino S, Kubo S, Umemoto R, Huang SX, Nishida N, et al. 2009. Observation of NMR signals from proteins introduced into living mammalian cells by reversible membrane permeabilization using a pore-forming toxin, streptolysin O. *J. Am. Chem. Soc.* 131:10834–35

116. Mittermaier AK, Kay LE. 2009. Observing biological dynamics at atomic resolution using NMR. *Trends Biochem. Sci.* 34:601–11

117. Milov AD, Ponomarev AB, Tsvetkov YD. 1984. Electron–electron double resonance in electron spin echo: model biradical systems and the sensitized photolysis of decalin. *Chem. Phys. Lett.* 110:67–72

118. Schiemann O, Prisner TF. 2007. Long-range distance determinations in biomacromolecules by EPR spectroscopy. *Q. Rev. Biophys.* 40:1–53

119. Jeschke G, Polyhach Y. 2007. Distance measurements on spin-labelled biomacromolecules by pulsed electron paramagnetic resonance. *PCCP* 9:1895–910

120. Krstić I, Hänsel R, Romainczyk O, Engels JW, Dötsch V, et al. 2011. Long-range distance measurements on nucleic acids in cells by pulsed EPR spectroscopy. *Angew. Chem. Int. Ed.* 50:5070–74

121. Igarashi R, Sakai T, Hara H, Tenno T, Tanaka T, et al. 2010. Distance determination in proteins inside *Xenopus laevis* oocytes by double electron–electron resonance experiments. *J. Am. Chem. Soc.* 132:8228–29

122. Witte C, Schröder L. 2013. NMR of hyperpolarised probes. *NMR Biomed.* 26:788–802

123. Lampel G. 1968. Nuclear dynamic polarization by optical electronic saturation and optical pumping in semiconductors. *Phys. Rev. Lett.* 20:491–93

124. Spence MM, Rubin SM, Dimitrov IE, Ruiz EJ, Wemmer DE, et al. 2001. Functionalized xenon as a biosensor. *PNAS* 98:10654–57

125. Goodson BM. 2002. Nuclear magnetic resonance of laser-polarized noble gases in molecules, materials, and organisms. *J. Magn. Reson.* 155:157–216

126. Schröder L. 2013. Xenon for NMR biosensing—inert but alert. *Phys. Med.* 29:3–16

127. Wolber J, Cherubini A, Leach MO, Bifone A. 2000. Hyperpolarized $^{129}$Xe NMR as a probe for blood oxygenation. *Magn. Reson. Med.* 43:491–96

128. Boutin C, Stopin A, Lenda F, Brotin T, Dutasta JP, et al. 2011. Cell uptake of a biosensor detected by hyperpolarized $^{129}$Xe NMR: the transferrin case. *Bioorg. Med. Chem.* 19:4135–43

129. Brotin T, Dutasta JP. 2009. Cryptophanes and their complexes—present and future. *Chem. Rev.* 109:88–130

130. Wei Q, Seward GK, Hill PA, Patton B, Dimitrov IE, et al. 2006. Designing $^{129}$Xe NMR biosensors for matrix metalloproteinase detection. *J. Am. Chem. Soc.* 128:13274–83

131. Chambers JM, Hill PA, Aaron JA, Han Z, Christianson DW, et al. 2009. Cryptophane xenon-129 nuclear magnetic resonance biosensors targeting human carbonic anhydrase. *J. Am. Chem. Soc.* 131:563–69

132. Seward GK, Bai Y, Khan NS, Dmochowski IJ. 2011. Cell-compatible, integrin-targeted cryptophane-$^{129}$Xe NMR biosensors. *Chem. Sci.* 2:1103–10

133. Schlundt A, Kilian W, Beyermann M, Sticht J, Günther S, et al. 2009. A xenon-129 biosensor for monitoring MHC-peptide interactions. *Angew. Chem. Int. Ed.* 48:4142–45

134. Rose HM, Witte C, Rossella F, Klippel S, Freund C, et al. 2014. Development of an antibody-based, modular biosensor for $^{129}$Xe NMR molecular imaging of cells at nanomolar concentrations. *PNAS* 111:11697–702

135. Palaniappan KK, Ramirez RM, Bajaj VS, Wemmer DE, Pines A, et al. 2013. Molecular imaging of cancer cells using a bacteriophage-based $^{129}$Xe NMR biosensor. *Angew. Chem. Int. Ed.* 52:4849–53

136. Bowers CR, Weitekamp DP. 1986. Transformation of symmetrization order to nuclear-spin magnetization by chemical reaction and nuclear magnetic resonance. *Phys. Rev. Lett.* 57:2645–48

137. Adams RW, Aguilar JA, Atkinson KD, Cowley MJ, Elliott PI, et al. 2009. Reversible interactions with para-hydrogen enhance NMR sensitivity by polarization transfer. *Science* 323:1708–11

138. Abraham M, McCausland MAH, Robinson FNH. 1959. Dynamic nuclear polarization. *Phys. Rev. Lett.* 2:449–51

139. Abragam A, Goldman M. 1978. Principles of dynamic nuclear polarisation. *Rep. Prog. Phys.* 41:395–467

140. Li C, Liu M. 2013. Protein dynamics in living cells studied by in-cell NMR spectroscopy. *FEBS Lett.* 587:1008–11

141. Li C, Tang C, Liu M. 2013. Protein dynamics elucidated by NMR technique. *Protein Cell* 4:726–30

# ANNUAL REVIEWS
## Connect With Our Experts
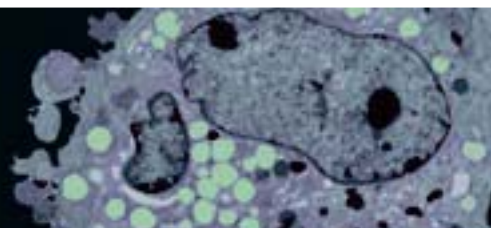
**ONLINE NOW!**

**New From Annual Reviews:**

## *Annual Review of Cancer Biology*
cancerbio.annualreviews.org · Volume 1 · March 2017

Co-Editors: **Tyler Jacks**, *Massachusetts Institute of Technology*

**Charles L. Sawyers**, *Memorial Sloan Kettering Cancer Center*

The *Annual Review of Cancer Biology* reviews a range of subjects representing important and emerging areas in the field of cancer research. The *Annual Review of Cancer Biology* includes three broad themes: Cancer Cell Biology, Tumorigenesis and Cancer Progression, and Translational Cancer Science.

**ANNUAL REVIEWS | CONNECT WITH OUR EXPERTS**

650.493.4400/800.523.8635 (US/CAN)
www.annualreviews.org | service@annualreviews.org

# Contents

Errata

An online log of corrections to *Annual Review of Analytical Chemistry* articles may be
found at http://www.annualreviews.org/errata/anchem